BİTLİS EREN ÜNİVERSİTESİ
FEN BİLİMLERİ DERGİSİ

ISSN: 2147-3129 / e-ISSN: 2147-3188

Article Type : Research Article
Received : June 18, 2025
Revised : September 11, 2025
Accepted : September 26, 2025
DOI : 10.17798/bitlisfen.1745357

Year : 2025
Volume : 14
Issue : 3
Pages : 1980-1995

INVESTIGATING EARTHQUAKE SOURCE SCALING LAWS IN THE AKHISAR SEISMIC ZONE

Alper DEMİRCİ [1]

[1] *Çanakkale Onsekiz Mart University, Geophysical Engineering Department, Çanakkale, Türkiye, alperdemirci@comu.edu.tr*

ABSTRACT

Spectral earthquake source parameters like corner frequency, fmax, stress drop and source radius are important parameters in terms of an earthquake's source properties. In this study, the source parameters of 40 local earthquakes (3.5≤M≤5.0) were calculated using Matlab-based codes. From 2011 to 2017 a database belonging to broadband earthquake stations for earthquakes occured near the location of the 12 September 2016 Akhisar (Manisa) earthquake was created from the Kandilli Observatory and Earthquake Research Institute seismic station network. Displacement and acceleration spectra including P and SH waves were analysed with a Brune ω^{-2} source model. A total of 40 earthquakes had 1097 waveforms investigated and parameters belonging to each earthquake were manually calculated. For each source parameter, mean values were calculated according to the number of seismic stations used for each earthquake. Observational spectra had damping effect removed using the Qs quality factor previously determined for the region. Seismic moment values obtained for the earthquakes varied from 0.19×10^{15} and 36.19×10^{15} Nm ($3.5 \leq Mw \leq 5$) with corner frequency values from 1.01 Hz to 5.07 Hz for P phase and 0.69 Hz to 2.63 Hz for SH phase. Additionally, calculations for SH phase in a circular fracture area varied from 0.72 km^2 to 11.12 km^2, with analyses of P phase calculated from 0.4 km^2 to 9.42 km^2. Noting the two phase calculations, the stress drop of the sources appeared to vary from 0.02 Mpa to 1.37 Mpa. In conclusion, these source parameters calculated at local scale revealed empirical relation functions with great importance to represent the region and as input for other scientific studies and were compared with results obtained from other similar studies in the literature.

Keywords: Corner frequency, Seismic Moment, Source Radius, Spectral Source Parameters, Stress Drop

1 INTRODUCTION

Earthquake source parameters and the relation functions between these parameters have great importance in revealing the kinematic and dynamic properties of the earthquake source. These parameters are commonly used in scaling relationship calculations for seismic risk analyses [1,2,3,4,5,6]. As understood from the Gutenberg-Richter scale [7], large earthquakes at global or local scale occur more rarely than moderate or low energy earthquakes. It is possible to research source functions for previously occurring large earthquakes by digitizing old analog earthquake records and analysing them. This situation brings with it many technical problems. As a result, small and moderate degree seismic events form the basis of the most important data source to identify relative uncertainties in both large and small events, to estimate the effect of large events and for seismic risk studies. As a result, increasing technological developments in recent years in seismic source theory make it possible to reveal the physical characteristics of a source reliably by calculation of parameters like seismic moment, stress drop and source radius considering the spectral characteristics of object waves for all micro and macro scale seismic events (e.g. [8]). Scientific studies on this topic by earth scientists increase every day. For example, when an earthquake occurs, a certain amount of stress energy is released and a sudden stress drop forms. The value of this stress drop ($\Delta\sigma$) is a parameter that should be calculated on a regional basis as it contains effects of the earthquake source at local scale. Thus, scaling the relationship between this and a variety of similar source parameters provides important clues to understand the source process. The relationship between corner frequency (fc) and seismic moment (M_0) especially has been researched by many researchers. Aki [9] revealed that theoretically for large earthquakes the two parameters should have $M_0 \sim fC^{-3}$ relationship. Lio [10] revealed that for relatively lower seismic moment values ($M_0 < 10^{15}$ Nm), this relationship was around $M_0 \sim fC^{-4}$ and stated that the incompatibility of scaling relationships between large and small earthquakes was due to differences in the rupture process. Apart from these parameters, scaling relationships provide important contributions to calculating low error rates for parameters like stress drop and source radius which are necessary to be able to identify the effects of possible strong ground motion in a region, in other words for modelling. According to variable tectonism and faulting character, these relationships have their own specific variable form for each region. As a result, using regional earthquake databases instead of current global correlations to reveal the regional scaling correlations and the rapid identification of these parameters and their use as an input for earthquake risk studies becomes very important. Additionally, this study is the first to examine the Akhisar Fault, not just due to using spectral

source parameters for earthquake data occurring on this fault, but because no detailed seismologic and seismotectonic study has been completed in this area.

The equations forming the basis and contributing to development of these types of studies were first determined by Brune [11]. Brune recommended a model to calculate source parameters using displacement amplitude spectra in close and distant areas as a function of the physical parameters of the source. Abercrombie and Leary [12] are researchers who provided significant contributions to the field of source parameter studies in recent times for a variety of locations on earth. Sharma and Wason [13] calculated the spectral source parameters for the Himalayas and surrounding regions.

In this study spectral analyses were completed using data from B.U. Kandilli Observatory and Earthquake Research Institute (KOERI) Regional Earthquake-Tsunami Monitoring and Evaluation Center [14] belonging to the 12.09.2016 Akhisar earthquake and events occurring before and after the earthquake around the epicenter area and obtained source parameters. These source parameters were correlated with each other in terms of representing the regional seismicity and the regional empirical relation functions were determined.

2 TECTONIC SETTINGS OF THE STUDY AREA

The study area was determined as 38.50 – 39.20 North latitude and 27.50 – 28.20 East longitude. This area is located within the Aegean Graben system (Figure 1). The Aegean Graben system represents one of the most active systems globally in terms of seismic activity showing the rapid expansion. The topic of this study, based on earthquakes occurring in the Akhisar Basin located within this active tectonism, is a 5.1 magnitude earthquake occurring on 12.09. 2016 at 11.26 at the intersection of 3 fault zones of the NNW-SSE oriented Soma-Kırkağaç Fault Zone, the 40 km long NNE-SSE right lateral strike-slip Akhisar-Sındırgı Fault Zone and the 35-40 km long NW-SE oriented Akhisar-Akselendi-Gölmarmara Fault Zone [15]. The distribution of aftershocks occurring after this earthquake continued and formed a NNW-SSE lineation. Koçyiğit et al. [16] in studies investigating the Akşehir Fault Zone stated the important fault zones in the region formed five separate regions from southeast to northwest with faults locking and making movement difficult and as a result forming a geometry that caused energy accumulation. One of these locking regions was stated to be around the Akhisar Fault Zone located west of Sındırgı. Kartal et al. [15] dealt with the tectonism in the region locally and obtained focal mechanism solutions showing left-lateral strike slip faulting and determined that the occurring earthquakes were due to rupture between two normal faults with opposite dips (Akselendi and Akhisar Faults).

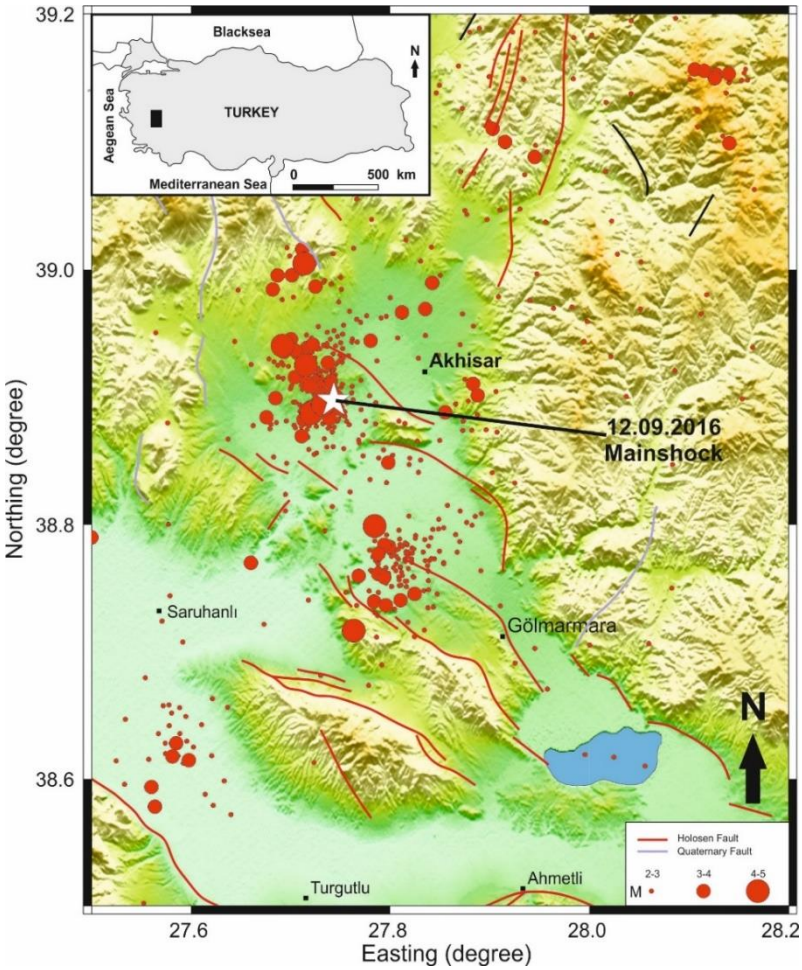


Figure 1. Active faults [17] and earthquakes occurred (M>2) in the study area between 2011 and 2017.

3 MATERIAL AND METHOD

Observational displacement spectrum (u) is stated below.

$$U(w)=S(w)*G(w)*R(w)*I(w) \quad (1)$$

In the equation S(w) is the source spectrum, G(w) includes the geometric distribution, wave propagation pattern and damping effects. R(w) comprises the local ground amplification at the measurement station while I(w) represents the instrument response spectrum of the measurement station.

In this study with the aim of obtaining the source spectrum, firstly raw data from broadband earthquake stations operated by KOERI had the instrument effect removal processes completed using the pole-zero data for the relevant station. In the next stage, a rotation process was applied to horizontal components with the aim of obtaining the SH wave phase. For the P wave phase vertical components were used. Brune's [11] source model showed clear slope variations at larger frequency than the corner frequency values. With the aim of preventing this,

changes formed at high frequency especially acceleration and displacement spectra had the 2nd degree low-pass Butterworth filter applied as recommended by Boore [18]. The theoretical acceleration and displacement source spectra as determined by Brune [11] are given in equations 2 and 3, respectively.

$$A(R,f) = \frac{C\omega^2\Omega_0}{1+(\frac{f}{f_c})^2} \tag{2}$$

$$D(R,f) = \frac{C\Omega_0}{1+(\frac{f}{f_c})^2} \tag{3}$$

In earthquake source models in the acceleration spectrum, the increase is fixed for a certain frequency interval until the corner frequency value, with transition to decreasing trend at different frequency values defined by Hanks [19]. This frequency value is named fmax. There are different opinions about this source of this value. Hanks [19] and Anderson and Hough [20] state this value is affected by local ground conditions, while Papageorgiou and Aki [21,22] and Yokai and Irikura [23] associated the fmax value with the source effect [24].

Especially in acceleration spectra, the frequency values equivalent to sharp slope changes like fc and fmax become clearer and their distinctiveness is more obvious. As a result, on the obtained acceleration spectra, the fc value was chosen as the frequency value where the spectrum amplitude increases suddenly, while the fmax value is the frequency value where the curve begins to fall again after continuing at stable level for a while. In light of this information, the fc, fmax and Ω0 (low frequency displacement spectral level) were manually determined on the acceleration spectrum (Figure 2).

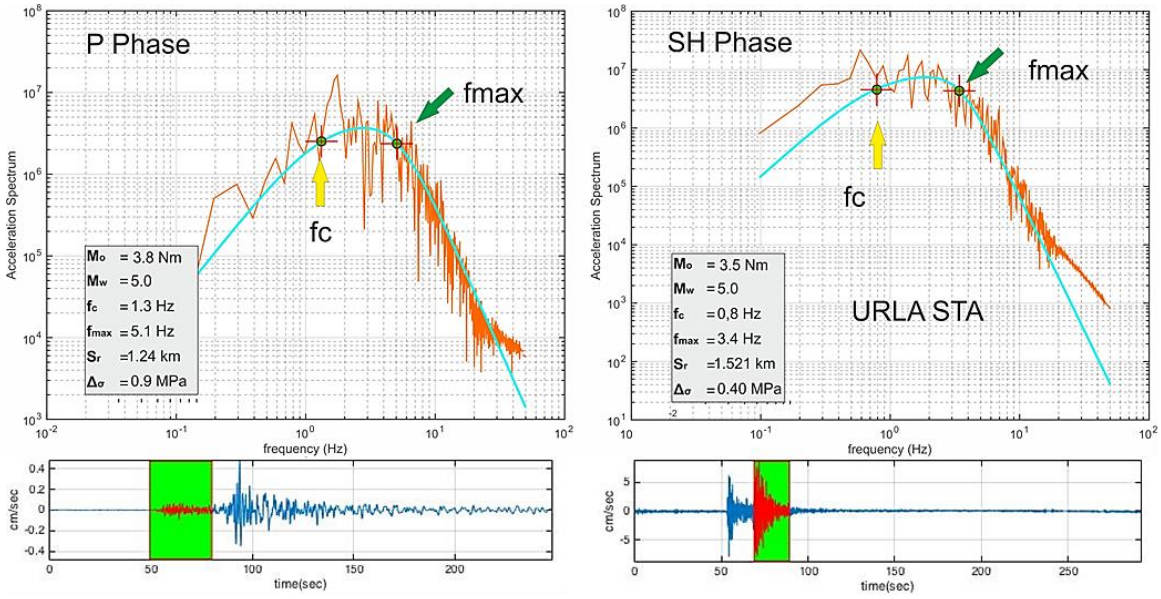


Figure 2. Two different phase spectral curves using URLA station data. Corner frequencies and calculated source parameters. (M_o will be multiplied by 10^{16})

In the next stage the previously calculated frequency-linked damping quality factor (Qsh) calculated for the region including the study area by Kurtulmuş and Akyol [25] was used with $Qsh=113.45f^{0,47}$ equation for distant stations (120-200 km) and $Qsh=60.97f^{1,42}$ equation for close stations (10-70 km). In this stage of spectral analysis, P wave phase Qp=2,25Qs assumption was applied (e.g., [26]). Using the chosen fc, fmax and Ω0 spectral parameters, the spectral curves belonging to the Brune source model calculated in equations 2 and 3 were overlaid with the observational spectra. Using the synthetic model determined with the trial and error method and representing lowest error of the observational curve, the source parameters like seismic moment, stress drop and source radius were obtained with the aid of the following equations.

$$M_0 = \frac{4\pi\rho\beta^3 R\Omega_0}{R_{\theta\varphi}S_a} \tag{4}$$

In the equation, M_0 is seismic moment, ρ is mean density value, β is mean shear wave velocity around the source, R is the distance from the hypocenter, $R_{\theta\varphi}$, is mean propagation pattern value and S_a represents the free surface ground amplification factor. After obtaining the seismic moment, the moment magnitude value (Mw) may be calculated with the aid of empirical equations developed by Hanks and Kanamori [27].

$$M_w = 0.66.log\, M_0 + 10.7 \tag{5}$$

The source radius (Sr) and stress drop (Δσ) parameters were calculated from equations 6 and 7.

$$S_r = \frac{K\beta}{2\pi f_c} \tag{6}$$

$$\Delta\sigma = \frac{7M_0}{16{s_r}^3} \tag{7}$$

The K constant used in source radius calculations was taken as 2.34 for calculations with the SH wave phase and as 1.92 for calculations with the P wave phase [28].

When the equations above are investigated, it may be said the obtained and calculated spectral source parameters have a linear and/or inverse correlation with each other. However, as the source radius and seismic moment are completely independent parameters it is important to correlate these two parameters, especially, with a range of regression analyses.

With the aim of minimizing the probable errors for 40 different earthquakes with moment magnitudes ranging between 3.5 and 5.0 occurred in the study area, the above calculations were completed using the mean results obtained for stations with high signal/noise

ratio taking note of azimuthal distribution. Due to the high data quality belonging to the main shock on 12.09.2016 and it being recorded at distant stations, this earthquake was analysed using SH phase data from 19 stations and P phase data from 21 stations. The stations used for main shock analysis and the spectral curves belonging to the SH wave phase are shown in Figure 3.

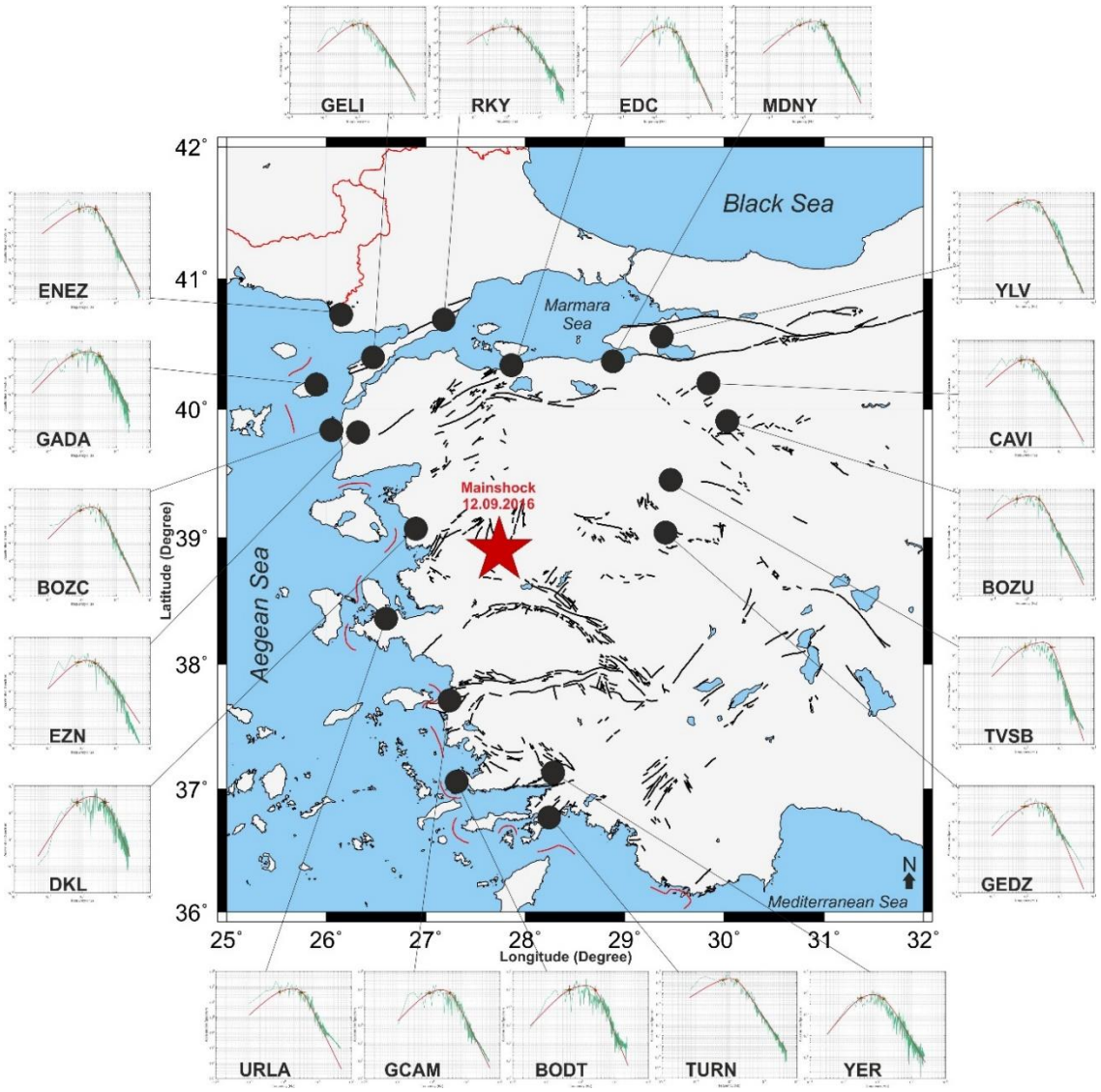


Figure 3. Stations used in spectral source analysis and observed SH wave phase spectra at these stations for 12.09.2016 earthquake

4 RESULTS AND DISCUSSIONS

The character of earthquake spectra and especially the scaling of this character with earthquake magnitude has great importance for engineering-based strong and weak motion simulation studies. With this aim in the scope of the study, the spectral source parameters belonging to 40 local earthquakes with magnitudes from 3.5 to 5.0 occurred near Akhisar (Western Anatolia) were separately calculated for the SH and P wave phases. It is an

unavoidable reality that the obtained results contain a certain amount of error due to the heterogeneity of the fault zone and the 1-D crustal model used in calculations. As a result, in the study, data from more than one station was used for each earthquake and the results obtained from the stations were taken as mean for each parameter in an attempt to reduce possible errors to a minimum. After completing the necessary corrections (damping response, instrument response, etc.), the obtained source spectrum curves were overlain with the Brune ω^{-2} source model with the aim of calculating parameters reflecting the source character (stress drop, corner frequency, seismic moment and source radius). The obtained source parameters for two different wave phases are given in Table 1 and Table 2.

Table 1. Spectral source parameters obtained using SH phase

Date	Tıme (UTM)	Lat	Long	Depth (km)	Mw	M_0 ($x10^{15}$Nm)	Fc (Hz)	Fmax (Hz)	Sd (Mpa)	Sr (m)	RA (km^2)	Nsta
06.10.2011	22:47:05	39.09	28.36	15.8	4.6	8.87	1.17	5.88	0.44	1055	3.50	5
04.08.2011	09:15:51	38.88	27.70	4.7	3.5	0.23	2.48	4.48	0.09	481	0.73	4
25.08.2011	10:45:27	38.96	27.60	8.6	3.8	0.64	1.86	5.35	0.11	649	1.32	7
08.02.2012	19:57:26	39.23	27.84	8.9	4.2	2.37	1.20	3.78	0.12	1010	3.20	8
03.08.2012	10:18:20	38.70	28.03	7.4	4.6	10.15	0.99	3.17	0.29	1240	4.83	11
04.08.2012	02:23:50	38.68	28.05	8.9	4.2	1.99	1.26	3.79	0.13	1010	3.20	6
04.08.2012	02:30:28	38.69	28.06	6.2	3.6	0.33	2.35	6.48	0.12	512	0.82	4
07.08.2012	23:17:37	38.70	28.06	9.7	4.1	1.80	1.30	3.84	0.10	918	2.65	6
07.08.2012	23:57:37	38.69	28.06	10.6	4.1	1.53	0.97	3.81	0.04	1258	4.97	9
25.08.2012	07:24:46	38.66	27.97	4.5	3.9	0.91	1.28	4.19	0.05	936	2.75	6
17.03.2013	14:03:04	39.28	27.84	8	3.9	0.69	1.37	3.93	0.05	895	2.52	7
24.05.2013	05:18:57	38.89	27.68	14	3.9	0.83	1.40	5.34	0.06	861	2.33	7
10.06.2013	16:36:03	39.01	27.86	6.8	3.5	0.24	1.72	3.93	0.03	701	1.54	5
25.06.2013	04:00:40	39.33	27.89	12.7	3.5	0.24	2.00	7.55	0.06	609	1.17	5
21.08.2013	14:54:18	38.71	27.93	9.4	3.7	0.37	1.85	6.18	0.06	648	1.32	5
12.11.2013	21:04:06	39.09	28.35	6.8	3.7	0.45	2.10	9.18	0.11	568	1.01	4
10.01.2014	21:33:13	38.81	27.81	12.4	3.7	0.36	1.69	4.36	0.05	719	1.62	7
02.06.2014	15:05:24	38.85	28.08	6.7	3.5	0.24	2.63	6.78	0.13	490	0.75	6
02.12.2015	15:52:44	39.15	28.14	14	3.8	0.51	2.14	7.19	0.17	583	1.07	9
13.12.2015	08:16:58	39.18	27.80	9.8	3.6	0.30	1.90	4.56	0.06	635	1.27	7
20.01.2016	06:07:44	39.10	27.91	7.7	3.6	0.33	1.45	5.46	0.03	860	2.32	8
03.07.2016	18:05:43	38.78	27.79	12.3	4.1	1.65	1.17	3.93	0.07	1042	3.41	7
12.09.2016	08:26:04	38.90	27.74	14	5.0	34.35	0.69	2.98	0.36	1882	11.13	19
12.09.2016	09:29:37	38.89	27.73	13.1	4.6	8.59	0.92	3.78	0.34	1338	5.62	7
15.09.2016	08:15:42	38.91	27.72	12.4	3.8	0.56	1.64	4.47	0.07	768	1.85	8
16.09.2016	07:23:23	38.88	27.68	6.1	3.6	0.27	1.61	3.70	0.03	762	1.82	6
17.09.2016	12:53:33	38.90	27.73	10.8	3.8	0.70	1.55	3.93	0.09	805	2.04	5
18.09.2016	22:48:24	38.90	27.68	8.4	3.7	0.39	1.72	4.85	0.06	717	1.62	6
19.09.2016	06:25:50	38.89	27.73	12.6	3.5	0.19	1.63	5.33	0.03	755	1.79	5
21.09.2016	14:56:51	38.91	27.72	7.7	3.7	0.38	1.46	4.65	0.04	865	2.35	8
22.09.2016	21:30:05	39.00	27.69	7.7	3.8	0.58	1.41	4.08	0.05	864	2.35	7
25.09.2016	20:51:20	38.90	27.73	12.7	4.0	1.01	1.37	4.36	0.08	898	2.53	6
09.10.2016	06:21:00	39.00	27.71	11.7	4.0	1.19	1.21	4.20	0.06	1002	3.15	9
15.10.2016	02:49:15	38.93	27.72	11.3	4.3	2.94	1.29	3.92	0.20	965	2.93	8
15.10.2016	02:51:03	38.94	27.69	6.3	4.4	4.27	1.13	3.53	0.17	1079	3.66	8
15.10.2016	03:02:28	38.92	27.70	8.3	3.7	0.43	1.52	4.69	0.04	793	1.98	5
15.10.2016	04:52:09	38.95	27.70	6.5	3.7	0.42	1.19	4.84	0.02	1038	3.38	6
15.10.2016	05:03:24	38.93	27.71	7.1	3.6	0.37	1.41	5.94	0.03	921	2.66	8
15.10.2016	22:23:23	38.94	27.70	8.2	3.7	0.46	1.22	4.69	0.02	995	3.11	8
15.10.2016	22:35:29	38.94	27.69	7.6	3.8	0.50	1.32	5.13	0.04	1001	3.15	7

Table 2. Spectral source parameters obtained using P phase

Date	Tıme (UTM)	Lat	Long	Depth (km)	Mw	M_0 ($x10^{15}$Nm)	Fc (Hz)	Fmax (Hz)	Sd (Mpa)	Sr (m)	RA (km^2)	Nsta
06.10.2011	22:47:05	39.09	28.36	15.8	4.6	9.60	2.04	6.46	1.37	1005	3.17	7
04.08.2011	09:15:51	38.88	27.70	4.7	3.8	0.83	2.94	5.30	0.15	726	1.66	3
25.08.2011	10:45:27	38.96	27.60	8.6	3.8	0.52	2.41	6.78	0.10	698	1.53	8
08.02.2012	19:57:26	39.23	27.84	8.9	4.2	2.15	2.57	5.48	0.42	671	1.41	6
03.08.2012	10:18:20	38.70	28.03	7.4	4.6	10.54	1.70	5.02	0.70	942	2.79	8
04.08.2012	02:23:50	38.68	28.05	8.9	4.2	2.12	2.04	5.86	0.96	974	2.98	8
04.08.2012	02:30:28	38.69	28.06	6.2	3.7	0.41	3.53	10.53	0.20	489	0.75	4
07.08.2012	23:17:37	38.70	28.06	9.7	3.9	0.94	1.82	4.07	0.09	1066	3.57	5
07.08.2012	23:57:37	38.69	28.06	10.6	4.1	1.79	3.10	6.73	1.09	614	1.18	6
25.08.2012	07:24:46	38.66	27.97	4.5	3.9	0.81	3.33	6.76	0.48	582	1.06	5
17.03.2013	14:03:04	39.28	27.84	8	3.8	0.59	2.29	8.24	0.12	765	1.84	7
24.05.2013	05:18:57	38.89	27.68	14	3.9	0.94	1.62	5.46	0.05	985	3.05	6
10.06.2013	16:36:03	39.01	27.86	6.8	3.5	0.35	2.90	6.36	0.09	603	1.14	6
25.06.2013	04:00:40	39.33	27.89	12.7	3.7	0.37	3.25	8.22	0.12	539	0.91	6
21.08.2013	14:54:18	38.71	27.93	9.4	3.7	0.41	4.05	6.82	0.35	434	0.59	6
12.11.2013	21:04:06	39.09	28.35	6.8	3.8	0.48	5.07	9.47	0.79	359	0.40	4
10.01.2014	21:33:13	38.81	27.81	12.4	3.7	0.44	2.72	5.22	0.09	627	1.24	7
02.06.2014	15:05:24	38.85	28.08	6.7	3.5	0.21	4.82	8.35	0.24	370	0.43	4
02.12.2015	15:52:44	39.15	28.14	14	3.8	0.63	3.10	6.38	0.22	551	0.95	7
13.12.2015	08:16:58	39.18	27.80	9.8	3.6	0.32	4.70	9.46	0.48	405	0.52	5
20.01.2016	06:07:44	39.10	27.91	7.7	3.6	0.31	3.76	8.88	0.17	459	0.66	4
03.07.2016	18:05:43	38.78	27.79	12.3	4.1	1.60	2.29	6.28	0.27	776	1.89	7
12.09.2016	08:26:04	38.90	27.74	14	5.0	36.19	1.01	4.58	0.45	1732	9.42	21
12.09.2016	09:29:37	38.89	27.73	13.1	4.6	8.25	1.11	4.51	0.27	1648	8.53	9
15.09.2016	08:15:42	38.91	27.72	12.4	3.8	0.65	2.82	5.44	0.15	587	1.08	7
16.09.2016	07:23:23	38.88	27.68	6.1	3.6	0.27	2.86	6.25	0.07	582	1.06	5
17.09.2016	12:53:33	38.90	27.73	10.8	3.9	0.85	2.19	4.93	0.10	765	1.84	4
18.09.2016	22:48:24	38.90	27.68	8.4	3.7	0.43	3.14	5.72	0.13	527	0.87	5
19.09.2016	06:25:50	38.89	27.73	12.6	3.6	0.28	3.61	7.63	0.13	472	0.70	5
21.09.2016	14:56:51	38.91	27.72	7.7	3.7	0.43	2.90	6.91	0.12	584	1.07	6
22.09.2016	21:30:05	39.00	27.69	7.7	3.9	0.81	2.35	5.28	0.11	716	1.61	7
25.09.2016	20:51:20	38.90	27.73	12.7	4.0	1.23	2.38	6.79	0.18	710	1.58	6
09.10.2016	06:21:00	39.00	27.71	11.7	4.1	1.55	1.84	6.63	0.11	960	2.90	9
15.10.2016	02:49:15	38.93	27.72	11.3	4.3	3.09	2.09	5.80	0.32	825	2.14	6
15.10.2016	02:51:03	38.94	27.69	6.3	4.5	6.65	1.67	5.05	0.35	1108	3.86	7
15.10.2016	03:02:28	38.92	27.70	8.3	3.8	0.63	2.86	6.67	0.16	588	1.09	7
15.10.2016	04:52:09	38.95	27.70	6.5	3.7	0.44	2.65	6.71	0.09	649	1.32	6
15.10.2016	05:03:24	38.93	27.71	7.1	3.7	0.51	3.02	7.67	0.14	552	0.96	8
15.10.2016	22:23:23	38.94	27.70	8.2	3.9	0.81	2.71	6.81	0.17	618	1.20	7
15.10.2016	22:35:29	38.94	27.69	7.6	3.8	0.61	2.45	7.04	0.11	690	1.50	6

Accordingly, for the earthquakes included in the study;

- Seismic moment values; for SH phase are between 0.23 - 34.35 ($x10^{15}$ Nm)
  for P phase are between 0.21 - 36.19 ($x10^{15}$ Nm)
- Corner frequency values; for SH phase are between 0.69 - 2.63 Hz
  for P phase are between 1.01-5.07 Hz
- Stress drop values; for SH phase are between 0.03 - 0.44 Mpa
  for P phase are between 0.09-1.37 Mpa
- Source radius values; for SH phase are between 481 - 1882 m
  for P phase are between 370 -1732 m

In light of the obtained results, all results obtained from two different phases were compared and the relations between these parameters were revealed using exponential and logarithmic regression analyses. The controversial parameter of fmax value was associated with seismic moment together with corner frequency value and it was observed that both frequency values displayed variation with close slope values (Figure 4). In terms of enlightening the debate, it may be said the fmax parameter includes similar source effects to the fc parameter.

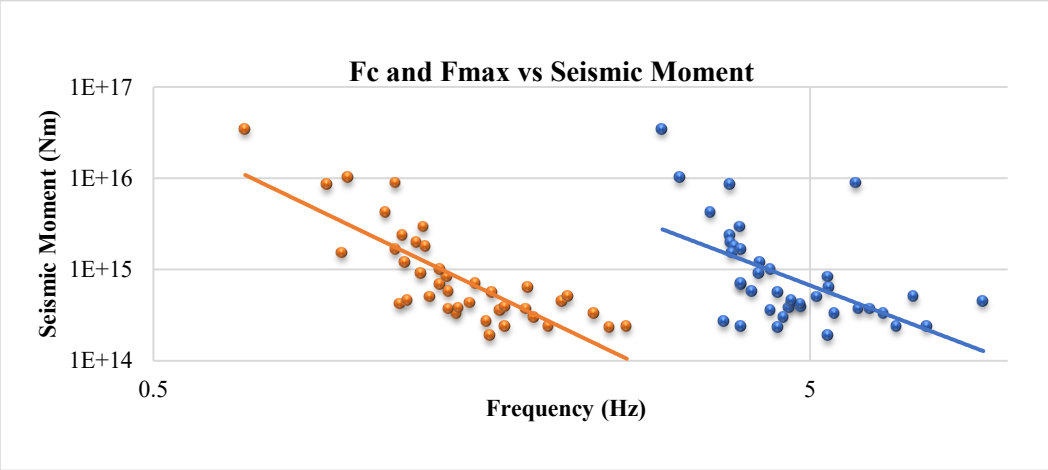


Figure 4. Variation in seismic moment of corner frequency and Fmax parameters

Firstly, the corner frequency (f_c) parameter has been dealt with by many researchers in different regions. Gusev et al. [29] stated the ratio obtained for corner frequency calculated from the P phase and S phase Fc (P) / Fc (S) should be about 1.4 for earthquakes in the shallow crust. This ratio was calculated as 1.5 by Lin et al. [30] and as 1.52 by Convertito et al. [31], while Ambeh and Fairhead [32] emphasized that this ratio may vary according to the geometry of the source model used. They observed this Fc(P) / Fc (S) ratio varied over a broad interval like 1.4±0.7 for different models, and stated this ratio approached 1 in linear source models especially (Haskell, etc.). Ambeh and Fairhead [32] revealed that in circular models this ratio should be close to the ratios of P and S wave velocities used in the crustal model. The corner frequency ratio obtained as a result of this study was calculated as 1.7 in accordance with the crustal model used [33] (Table 3).

Table 3. Crustal velocity model used in the study [33]

Depth (Km)	Vp (km/s)	Vs (km/s)	Vp / Vs
0.0	4.50	2.60	1.73
5.40	5.91	3.10	1.90
31.6	7.80	4.50	1.73
89.2	8.30	4.80	1.73

Additionally, corner frequency is associated with seismic moment in many studies (Table 4). Especially for the related function containing a range of information in terms of determining the type of source, Aki [9] revealed that theoretically these two parameters should have $M_0 \sim fC^{-3}$ correlation for large earthquakes. Lio [10] revealed that at relatively lower seismic moment values ($M_0 < 10^{15}$ Nm) this relationship is around $M_0 \sim fC^{-4}$ and stated the incompliance in scaling relationships between large and small earthquakes is due to differences in the rupture processes. In this study the correlation between the seismic moment and corner frequency was calculated as $Mo.fc^{3.46} = 3.10^{15}$ N-m/sec for the SH phase and as $Mo.fc^{2.7} = 10^{16}$ N-m/sec for the P phase.

Table 4. Related functions for different regions in the literature (seismic moment- corner frequency)

Ref.	Studied Region	Scaling Function
Watanabe et al. [34]	Kanto Basin (Japan)	$Mo.fc^3 = (2.5\text{-}3.0).10^{16}$ N-m/sec
Dutta et al [35]	South-Central Alaska	$Mo.fc^3 = 2.09.10^{16}$ N-m/sec
Kumar et al. [36]	Himalayan Region (India)	$Mo.fc^3 = 1.7.10^{16}$ N-m/sec
Kumar [37]	Garhwal Himalaya (India)	$Mo.fc^3 = 3.10^{16}$ N-m/sec
Borkar et al. [38]	Kumaun Himalaya (India)	$Mo.fc^{2.7} = 5.10^{16}$ N-m/sec
Yoo et al. [39]	Korean Peninsula	$Mo.fc^{3.54} = 10^{16}$ N-m/sec
Present Study	Akhisar Region (Western Türkiye)	$Mo.fc^{3.46} = 3.10^{15}$ N-m/sec (SH Phase)
Present Study	Akhisar Region (Western Türkiye)	$Mo.fc^{2.7} = 10^{16}$ N-m/sec (P Phase)

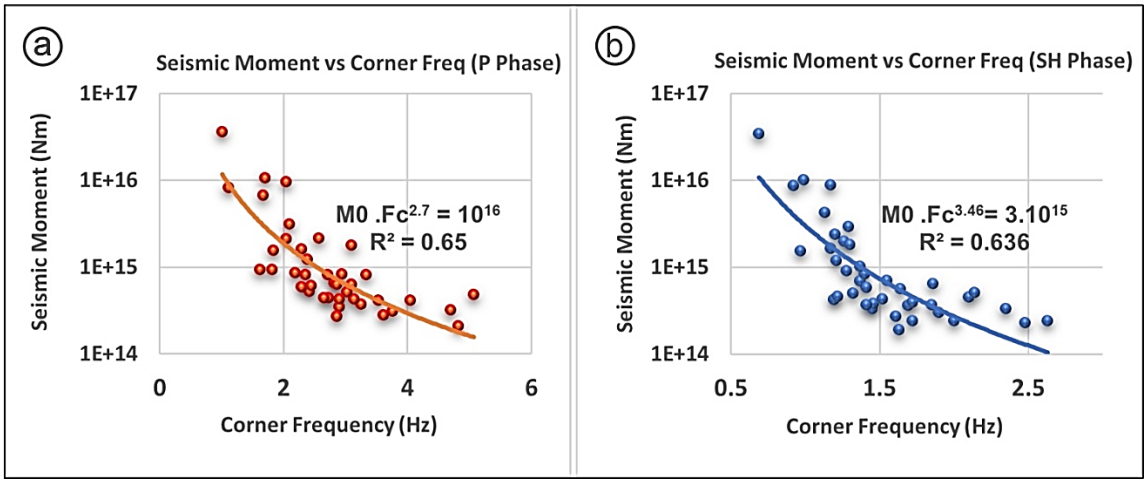


Figure 5. Graphs of relationship between seismic moment and corner frequencies a) P phase, b) SH phase

Similarly, another relation function mentioned in many studies is between the seismic moment and source radius parameters (Table 5). As seen in Figure 6, the relation function between these two parameters was calculated as $Log(M_0)= 3.36.log(r) + 5.06$ with regression coefficient of 0.63. The similarity with crustal model and with the scaling function ($Log(M_0)=3.38.log (r) + 4.79$) obtained for northwest Greece by Stavroulopoulou et al. [40] noted in Table 5 for areas close to the study area is one of the clear indicators that these types of functions represent regional character.

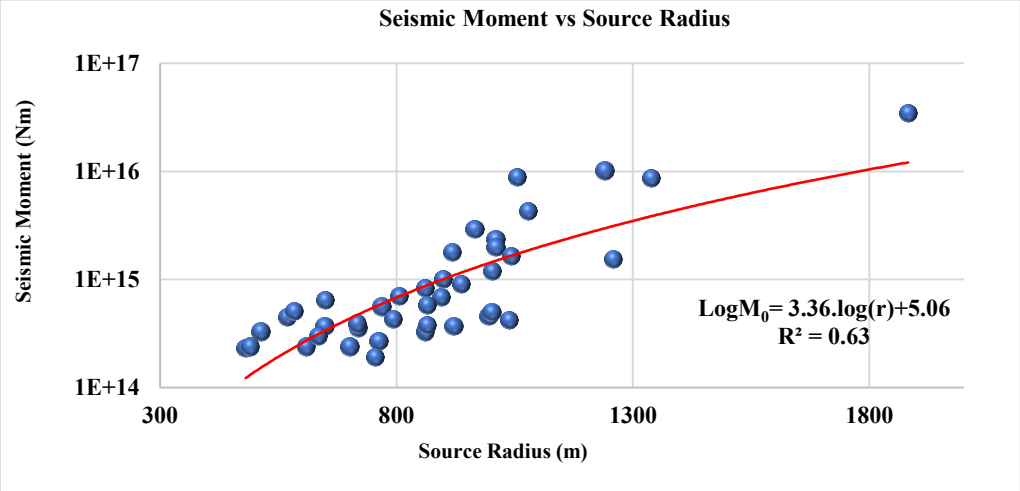


Figure 6. Graph of correlation between seismic moment and source radius

Table 5. Related functions for different regions in the literature (seismic moment and source radius)

Ref.	Studied Region	Scaling Function
Dobrynina [41]	Baikal Rift (Northern Eurasia)	$Log(M_0)\pm0.90= 8.85.log(r) + 15.16$
Sule and Weber [42]	Central Pannonian basin (Hungary)	$Log(M_0)= 4.76.log (r) + 1.62\pm2.05$
Sanoujam [43]	Manipur (India)	$Log(M_0)= 1.56.r + 13.68$
Popescu et al. [44]	Vrancea (Romania)	$Log(M_0) = 2.87\pm0.03.log(r) + 7.41\pm0.3$
Stavroulopoulou et al [40]	Epirus (Northwestern Greece)	$Log(M_0)= 3.38.log (r) + 4.79$
Mohamed [45]	Kalabsha (Egypt)	$Log(M_0) = 0.7\pm0.04.log(r) + 11.06\pm0.5$
Present Study	Akhisar Region (Western Türkiye)	$Log(M_0)= 3.36.log(r)+5.06$

It is noteworthy that the relation function between the stress drop and seismic moment ($Log (M_o)= 1.16.log (\Delta\sigma) + 16.22$) is more similar to the results obtained by Stavroulopoulou et al. [40] ($Log (M_0)= 1.11.log (\Delta\sigma) + 11.7$) compared to other studies (Table 6). As shown on Figure 6 and 7, as in studies comparing variations in stress drop and source radius linked to seismic moment, this only includes results from the SH phase.

Table 6. Related functions for different regions in the literature (seismic moment and stress drop)

Ref.	Studied Region	Scaling Function
Dobrynina [41]	Baikal Rift (Northern Eurasia)	$Log(M_0)\pm0.30= 1.26.log(\Delta\sigma) + 15.3$
Garcia-Garcia et al. [46]	Southern Spain	$Log(M_0)=1.1\pm0.17.log(\Delta\sigma)+19.47\pm0.09$
Radulian and Popa [47]	Vrancea (Romania)	$Log(M_0)= 3.7. log(\Delta\sigma) + 20.48$
Stavroulopoulou et al [40]	Epirus (Northwestern Greece)	$Log(M_0)= 1.11.log (\Delta\sigma) + 11.7$
Mohammed [45]	Kalabsha (Egypt)	$Log(M_0) = 0.44\pm0.19.log(\Delta\sigma) + 12.23\pm0.5$
Present Study	Akhisar Region (Western Türkiye)	$Log(M_0)= 1.16.log(\Delta\sigma) + 16.22$

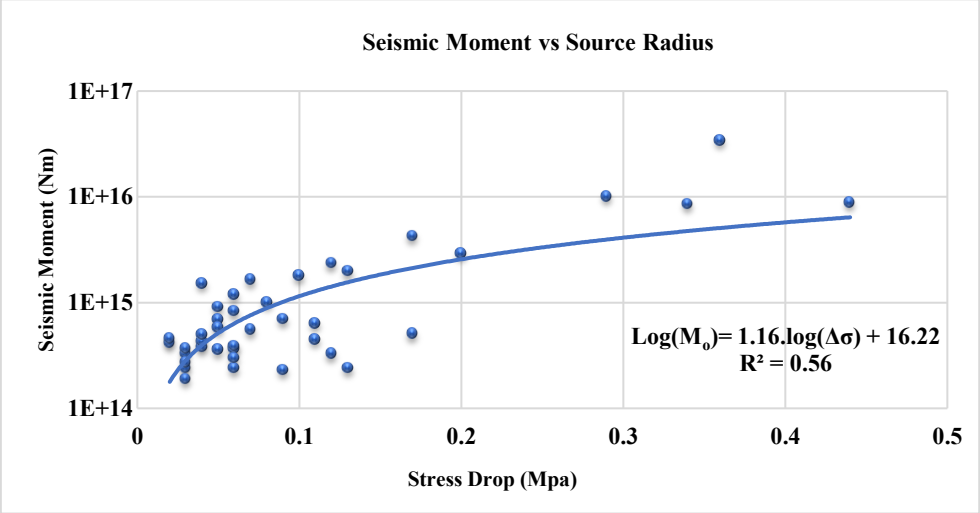


Figure 7. Graph of correlation between seismic moment and stress drop

5 CONCLUSIONS

The relation functions obtained in this study using small and moderate magnitude earthquake data from the region are an important reference in terms of being able to calculate the effects of possible large earthquakes in the region and close surroundings. The absence of prior comprehensive studies in this region highlights the significance of the derived scaling relationships, which may serve as essential input parameters for earthquake simulations, stress modeling, and other seismological applications in adjacent areas. Furthermore, this research closes a major gap by investigating the first detailed seismic source analysis for the Akhisar Basin. The resulting regional empirical relationship functions are vital inputs for assessing seismic hazards, ground motion simulations, and modeling future earthquake scenarios in Western Anatolia. Subsequent studies might expand the approach to include higher-magnitude events, fault-specific segmentation, and wider spatial data to test the scaling laws' generalizability. The established methodology is also applicable to similar intraplate regions lacking robust source characterization.

Acknowledgments

Analyses are performed by using modified form of Matlab –based EQK-SRC-PARA codes [24] and some figures were created with the Generic Mapping Tools of Wessel and Smith [48].

Statement of Research and Publication Ethics

The study is complied with research and publication ethics.

Artificial Intelligence (AI) Contribution Statement

This manuscript was entirely written, edited, analyzed, and prepared without the assistance of any artificial intelligence (AI) tools. All content, including text, data analysis, and figures, was solely generated by the author.

REFERENCES

[1] T. C. Hanks and M. Wyss, "Use of body-wave spectra in determination of seismic-source parameters," *Bull. Seismol. Soc. Amer.*, vol. 62, no. 2, pp. 561–589, Apr. 1972.

[2] T. C. Hanks and W. Thatcher, "Graphical representation of seismic source parameters," *J. Geophys. Res.*, vol. 77, no. 23, pp. 4393–4405, Dec. 1972.

[3] R. E. Abercrombie, "Earthquake source scaling relationships from 1 to 5 ML using seismograms recorded at 2.5 km depth," *J. Geophys. Res. Solid Earth*, vol. 100, no. B12, pp. 24015–24036, Dec. 1995.

[4] N. Akyol and Ö. Karagöz, "Empirical attenuation relationships for Western Anatolia, Turkey," *Turkish Journal of Earth Sciences*, vol. 18, no. 3, pp. 351–382, 2009.

[5] Demirci, T. Bekler, İ. B. Karaşin, and E. Işık, "Karlıova (Bingöl) üçlü birleşim noktasında spektral kaynak parametreleri," in *Proc. 1st Int. Multidisciplinary Studies Congr.*, Dec. 28–29, 2018.

[6] E. Gök, "Source parameters and scaling relations of local earthquakes from a strong motion network in Izmir, Western Turkey," *Pure Appl. Geophys.*, vol. 176, no. 8, pp. 3391–3409, 2019.

[7] B. Gutenberg and C. F. Richter, "Frequency of earthquakes in California," *Bull. Seismol. Soc. Amer.*, vol. 34, no. 4, pp. 185–188, Oct. 1944.

[8] H. Kanamori, "Importance of historical seismograms for geophysical research," in *Historical Seismograms and Earthquakes of the World*, W. H. K. Lee, H. Meyers, and K. Shimazaki, Eds. San Diego, CA, USA: Academic Press, 1988.

[9] K. Aki, "Scaling law of seismic spectrum," *J. Geophys. Res.*, vol. 72, no. 4, pp. 1217–1231, Feb. 1967.

[10] Y. Iio, "Scaling relation between earthquake size and duration of faulting for shallow earthquakes in seismic moment between 10^{10} and 10^{25} dyne/cm," *J. Phys. Earth*, vol. 34, pp. 127–169, 1986.

[11] J. N. Brune, "Tectonic stress and the spectra of seismic shear waves from earthquakes," *J. Geophys. Res.*, vol. 75, no. 26, pp. 4997–5009, Sep. 1970.

[12] R. E. Abercrombie and P. Leary, "Source parameters of small earthquakes recorded at 2.5 km depth, Cajon Pass, southern California: Implications for earthquake scaling," *Geophys. Res. Lett.*, vol. 20, no. 14, pp. 1511–1514, Jul. 1993.

[13] M. L. Sharma and H. R. Wason, "Occurrence of low stress drop earthquakes in the Garhwal Himalayan region," *Phys. Earth Planet. Interiors*, vol. 85, no. 3–4, pp. 265–272, 1994.

[14] KOERI Earthquake Catalog, Boğaziçi Univ., Kandilli Observatory and Earthquake Research Institute, National Earthquake Monitoring Center. [Online]. Available: http://www.koeri.boun.edu.tr/sismo/2/data-request/

[15] R. F. Kartal, R. Demirtaş, F. T. Kadirioğlu, and S. Zünbül, "12 Eylül 2016 Akhisar-Manisa depremleri (Mw=4.6, Mw=4.5)," in *Proc. 20th Active Tectonic Research Group Workshop*, Denizli, Türkiye, Oct. 13–15, 2016, p. 10. (in Turkish)

[16] Koçyiğit, E. Bozkurt, N. Kaymakcı, and F. Şaroğlu, "3 Şubat 2002 Afyon Çay depreminin kaynağı ve ağır hasarının nedenleri: Akşehir Fay Zonu," *Jeolojik Ön Rapor*, Ortadoğu Teknik Üniversitesi, Ankara, Türkiye, 2002, 19 pp. (in Turkish)

[17] Ö. Emre, T. Y. Duman, S. Özalp, H. Elmacı, Ş. Olgun, and F. Şaroğlu, *Açıklamalı Türkiye Diri Fay Haritası*. Ankara, Türkiye: Maden Tetkik ve Arama Genel Müdürlüğü, 2013.

[18] D. M. Boore, "Stochastic simulation of high-frequency ground motions based on seismological models of the radiated spectra," *Bull. Seismol. Soc. Amer.*, vol. 73, no. 6, pp. 1865–1894, Dec. 1983.

[19] T. C. Hanks, "fmax," *Bull. Seismol. Soc. Amer.*, vol. 72, no. 6, pp. 1869–1879, Dec. 1982.

[20] J. G. Anderson and S. E. Hough, "A model for the shape of the Fourier amplitude spectrum of acceleration at high frequencies," *Bull. Seismol. Soc. Amer.*, vol. 74, no. 5, pp. 1969–1993, Oct. 1984.

[21] S. Papageorgiou and K. Aki, "A specific barrier model for the quantitative description of inhomogeneous faulting and the prediction of strong ground motion – Part I: Description of the model," *Bull. Seismol. Soc. Amer.*, vol. 73, no. 3, pp. 693–722, Jun. 1983.

[22] S. Papageorgiou and K. Aki, "A specific barrier model for the quantitative description of inhomogeneous faulting and the prediction of strong ground motion – Part II: Applications of the model," *Bull. Seismol. Soc. Amer.*, vol. 73, no. 4, pp. 953–978, Aug. 1983.

[23] T. Yokai and K. Irikura, "Meaning of source-controlled fmax in empirical Green's function technique based on a T^2-scaling law," *Annu. Disas. Prev. Res. Inst., Kyoto Univ.*, vol. 34, no. B-1, 1991.

[24] Kumar, A. Kumar, H. Mittal, A. Kumar, and R. Bhardwaj, "Software to estimate earthquake spectral and source parameters," *Int. J. Geosci.*, vol. 3, pp. 1142–1149, 2012.

[25] T. Ö. Kurtulmuş and N. Akyol, "Crustal attenuation characteristics in western Türkiye," *Geophys. J. Int.*, vol. 195, no. 2, pp. 1384–1394, 2013.

[26] D. Gajewski, R. Stangl, K. Fuchs, and K. Sandmeier, "A new constraint on the composition of the topmost continental mantle: Anomalously different depth increases of P and S velocity," *Geophys. J. Int.*, vol. 103, pp. 497–507, 1990.

[27] T. C. Hanks and H. Kanamori, "A moment magnitude scale," *J. Geophys. Res.*, vol. 84, no. B5, pp. 2348–2350, May 1979.

[28] K. Sivaram, D. Kumar, and S. S. Teotia, "Source parameters and scaling relations for small earthquakes in Kumaon Himalaya, India," *J. Seismol.*, vol. 17, no. 3, pp. 579–592, 2013.

[29] Gusev, M. Radulian, M. Rizescu, and G. F. Panza, "Source scaling of intermediate-depth Vrancea earthquakes," *Geophys. J. Int.*, vol. 151, no. 3, pp. 879–889, 2002.

[30] Lin, T. Satsukawa, M. Wang, A. Z. Mohammadi, R. Fueta, and F. Nakajima, "Coseismic rupturing stopped by Aso volcano during the 2016 Mw 7.1 Kumamoto earthquakes," *Science*, vol. 354, no. 6314, pp. 869–875, Nov. 2016.

[31] V. Convertito, A. Zollo, N. Sharma, A. Orefice, and A. Emolo, "Earthquake source parameters and scaling relationships at The Geysers geothermal field, California," in *Proc. AGIS Workshop Induced Seismicity*, Davos, Switzerland, Mar. 10–30, 2015.

[32] W. B. Ambeh and J. D. Fairhead, "Spectral characteristics and source parameters of micro earthquakes from the Mt Cameroon volcanic region, West Africa," *Geophys. J. Int.*, vol. 106, no. 2, pp. 229–237, 1991.

[33] D. Kalafat, C. Gürbüz, and S. B. Üçer, "Batı Türkiye'de kabuk ve üst manto yapısının araştırılması," *Deprem Araştırma Bülteni*, vol. 59, pp. 43–64, 1987. (in Turkish)

[34] K. Watanabe, H. Sato, S. Kinoshita, and M. Ohtake, "Source characteristics of small to moderate earthquakes in the Kanto region, Japan: Application of a new definition of the S-wave time window length," *Bull. Seismol. Soc. Amer.*, vol. 86, no. 5, pp. 1284–1291, Oct. 1996.

[35] U. Dutta, N. Biswas, A. Martirosyan, A. Papageorgiou, and S. Kinoshita, "Estimation of earthquake source parameters and site response in Anchorage, Alaska, from the strong motion network data using generalized inversion method," *Phys. Earth Planet. Interiors*, vol. 137, pp. 13–29, 2003.

[36] D. Kumar, V. Sriram, I. Sarkar, and S. S. Teotia, "An estimate of a scaling law of seismic spectrum for earthquakes in Himalaya," *Indian Minerals*, vol. 61, no. 3–4, pp. 83–92, 2008.

[37] Kumar, "Study of earthquake source parameters using micro-earthquakes and strong motion data," Ph.D. dissertation, Indian Inst. Technol., Roorkee, India, 2011.

[38] Y. Borkar, A. Kumar, and S. C. Gupta, "Source parameters and scaling relation for local earthquakes in the Garhwal and Kumaun Himalaya, India," *Int. J. Adv. Seismol.*, vol. 1, no. 1, pp. 1–15, 2013.

[39] S. H. Yoo, J. R. Rhie, H. Choi, and K. Mayeda, "Coda-derived source parameters of earthquakes and their scaling relationships in the Korean Peninsula," *Bull. Seismol. Soc. Amer.*, vol. 101, no. 5, pp. 2388–2398, Oct. 2011.

[40] O. Stavroulopoulou, E. Sokos, and G. A. Tselentis, "S-wave spectral analysis and estimation of spectral parameters in Northwestern Greece," *Bull. Geol. Soc. Greece*, vol. 50, pp. 1232–1240, 2016.

[41] A. Dobrynina, "Source parameters of the earthquakes of the Baikal rift system," *Izv., Phys. Solid Earth*, vol. 45, no. 12, pp. 1093–1109, 2009.

[42] Süle and Z. Wéber, "Earthquake source parameters and scaling relationships in Hungary (central Pannonian basin)," *J. Seismol.*, vol. 17, no. 2, pp. 507–521, 2013.

[43] M. Sanoujam, "Seismotectonic studies in Manipur," Ph.D. dissertation, Manipur Univ., Manipur, India, 2002.

[44] E. Popescu, A. O. Placinta, F. Borleasnu, and M. Radulian, "Repeated earthquakes in the Vrancea subcrustal source and source scaling," *IOP Conf. Ser.: Earth Environ. Sci.*, vol. 95, p. 032005, 2017.

[45] H. H. Mohamed, "Determination of basic physical source parameters and scaling relations for Kalabsha earthquakes, Aswan, Egypt," *Acta Geodyn. Geomater.*, vol. 1, no. 2, pp. 201–212, 2004.

[46] J. M. García-García, M. D. Romacho, and A. Jiménez, "The corner frequencies, stress drops and apparent stresses of microearthquakes in the Betic region (Southern Spain)," *Física de la Tierra*, vol. 14, pp. 161–182, 2002.

[47] M. Radulian and M. Popa, "Scaling of source parameters for Vrancea (Romania) intermediate depth earthquakes," *Tectonophysics*, vol. 261, pp. 67–81, 1996.

[48] P. Wessel and W. H. F. Smith, "New version of generic mapping tools released," *EOS Trans. Amer. Geophys. Union*, vol. 76, p. 329, 1995.